University of Thi-Qar Journal of Science (UTJsci)
E-ISSN: 2709-0256, P-ISSN: 1991-8690, Vol. 12, No.2,Dec . 2025

Phyto-Mediated Route for Nickel Oxide Nanoparticle Synthesis Using *Microtrichia perotitii* DC Extract: Characterization and Antibacterial Activity

Friday Meshach Danjuma[1, 2a*], Bamigboye Mercy Oluwaseyi[2b], Owoyemi Wilfred Iyanuoluwa[2c], Oyabambi Atinuke[2d], Joshua Tunde Olaifa[3e], Miracle Oluwabukunmi Obaleye[4f]

[1]*Department of Science Laboratory Technology, Newland Polytechnic, Ilorin 240102, Kwara State Nigeria*

[2]*Department of industrial chemistry, Faculty of Physical Sciences, University of Ilorin, Kwara State, Nigeria*

[3]*Department of Crop Science, Faculty of Agriculture, University of Ilesa, Osun state, Nigeria*

[4]*Department of Microbiology, Faculty of Sciences, University of Ilesa, Osun state, Nigeria*

[b]Email: obaleye.mo@unilorin.edu.ng , [c]Email: owoyemiwilfred@gmail.com , [d]Email: oyabambiatinuke@gmail.com ,

[e]Email: Joshua_olaifa@unilesa.edu.ng , [f]Email: miracle_obaleye@unilesa.edu.ng

[a*]*Corresponding author*: Friday.md@newlandpolytechnic.edu.ng or meshachfridaydan@gmail.com

Received: 2025-10-20, Revised: 2025-11-27, Accepted: 2025-12-20, Published: 2025-12-28

Abstract*—The growing demand for sustainable nanomaterials has intensified interest in green synthesis routes utilizing plant-derived biomolecules as reducing and stabilizing agents. This study reports, for the first time, the biosynthesis of nickel oxide nanoparticles (NiO NPs) using *Microtrichia perotitii* DC leaf extract, a medicinal plant rich in bioactive phytochemicals including flavonoids, alkaloids, tannins, phenolics, and saponins. Nickel (II) chloride hexahydrate served as the metal precursor, while the phytochemicals facilitated both nanoparticle formation and stabilization. The synthesized NiO NPs were comprehensively characterized using UV-visible spectroscopy, Fourier-transform infrared spectroscopy (FTIR), X-ray diffraction (XRD), scanning electron microscopy (SEM) with energy-dispersive X-ray spectroscopy (EDX), and thermogravimetry/differential thermal analysis (TG/DTA). XRD analysis confirmed the formation of crystalline nanoparticles with an average crystallite size of 24 nm and a cubic bunsenite phase. FTIR spectroscopy revealed a characteristic Ni-O stretching vibration at 651 cm^{-1}, confirming successful NiO formation. SEM imaging showed irregular, agglomerated nanostructures, while TG/DTA analysis demonstrated good thermal stability with major decomposition occurring at 473°C, attributed to the removal of phytochemical residues. Antibacterial assays demonstrated strong inhibitory effects of the biosynthesized NiO NPs, particularly against Gram-positive bacteria, including *Bacillus subtilis* (18.8 ± 0.6 mm) and *Staphylococcus aureus* (19.6 ± 0.4 mm) at 100 µg/mL concentration. Although the activity was slightly lower than ciprofloxacin (5 µg/disc: 22.4 ± 0.5 mm and 23.1 ± 0.43 mm, respectively), it indicates significant antibacterial potential. Gram-negative strains exhibited comparatively lower sensitivity, likely due to their protective outer membrane barrier. This first report of *M. perotitii*-mediated NiO NP synthesis highlights the untapped potential of this indigenous West African plant for eco-friendly nanomaterial production and demonstrates the applicability of these nanoparticles in biomedical and environmental applications.

***Keywords*—Green synthesis, Nickel Oxide, Nanoparticles, *Microtrichia perotitii* DC, Characterization.**

I. INTRODUCTION

Nanoparticles have special physicochemical characteristics that have gained a lot of attention due to their surface area-to-volume ratio, tunable morphology, and unique optical, magnetic, and catalytic behaviors. Because of these properties, NPs can be used in a variety of fields, including biomedicine, environmental remediation, energy storage, and catalysis [1–3].

For the production of nanoparticles, traditional synthesis techniques like hydrothermal, sol–gel, microemulsion, electrospray, and laser ablation methods have been extensively used [4, 5]. However, there are issues with cytotoxicity and the environment because these physicochemical methods are frequently expensive, energy-intensive, and dependent on hazardous chemicals [6].

Green nanotechnology, on the other hand, has become a viable and environmentally beneficial substitute by using biological organisms like bacteria, fungi, algae, and plants as natural reducing and stabilizing agents [7–9]. The presence of phytochemicals (such as phenolics, flavonoids, alkaloids, tannins, and terpenoids) that act as bioreductants and capping agents, as well as its simplicity, affordability, and scalability, make plant-mediated synthesis stand out among these biological systems [10, 11]. Because these biomolecules improve the stability and biocompatibility of nanoparticles, plant-derived NPs hold great promise for use in environmental and biomedical applications.

The remarkable chemical stability, wide bandgap, high coercivity, magnetocrystalline anisotropy, large specific capacitance, and electrochemical durability of nickel oxide nanoparticles (NiO NPs) make them particularly interesting [12]. As a result, NiO NPs have been used in dye-sensitized solar cells, electrochemical sensors, supercapacitors, and catalysis [13–15]. The significance of creating sustainable synthesis pathways for these

https://doi.org/10.32792/utq/utjsci/v12i2.1503

multipurpose nanomaterials is further highlighted by the diverse biological properties of biologically synthesized NiO NPs, which include antioxidant, antibacterial, antifungal, anticancer, and enzyme inhibitory activities.

West African nations like Nigeria, Senegal, Guinea, Sierra Leone, Ivory Coast, and Ghana are home to the medicinal plant *Microtrichia perotitii* DC, which is a member of the Asteraceae family [16]. The presence of bioactive substances such as flavonoids, alkaloids, tannins, phenolics, and saponins has been verified by phytochemical studies. Because of its analgesic, anti-inflammatory, and antidiarrheal qualities, *M. perotitii* DC has been used historically [16]. Its use in the biosynthesis of NiO NPs has not yet been documented, despite its rich phytochemical composition.

A number of plant species have been investigated in the past for the environmentally friendly synthesis of NiO NPs. For instance, when examined by XRD, SEM, TGA, DSC, and FTIR analyses, NiO NPs made with leaf extract from Acacia nilotica demonstrated exceptional electrochemical and antibacterial qualities [17]. Similarly, it was confirmed that NiO NPs mediated by Vernonia amygdalina leaf extract had a bunsenite phase with an average crystallite size of 17.86 nm, octahedral morphology, and a noticeable Ni–O stretching vibration at 1094.8 cm^{-1} [18].

Nevertheless, it is still unclear how the phytochemical makeup of *M. perotitii* DC affects the nucleation, reduction, and stabilization of NiO NPs. We speculate that *M. perotitii* DC's phytoconstituents can efficiently convert nickel ions to NiO NPs while enhancing particle stability and biological activity because of the plant's high concentration of phenolic and flavonoid compounds.

As far as we are aware, this work is the first to describe the environmentally friendly synthesis of NiO NPs using leaf extract from *M. perotitii* DC. The structural, optical, and morphological characteristics of the produced nanoparticles were thoroughly described, and a systematic assessment of their antibacterial activity against both Gram-positive and Gram-negative pathogens was conducted. This study presents *M. perotitii* DC as a novel bio-resource for the synthesis of environmentally friendly nanomaterials, offering insights into the phytochemical-assisted bioreduction mechanism of the plant and laying the groundwork for a sustainable process for creating biocompatible NiO NPs with potential uses in the environment and in medicine.

II. MATERIALS AND METHODS.

A. *Chemicals and Reagents*

The materials used in this study included nickel (II) chloride hexahydrate, absolute ethanol, sodium hydroxide, phosphate buffer, sulfuric acid, nitric acid, chloroform, Wagner's solution, ferric chloride salts, concentrated HCl, ascorbic acid, deionized distilled water, and *M. perotitii* DC leaf. All chemicals and reagents were of analytical grade.

B. *Preparation of* M. perotitii *DC Leaf Extract*

The *M. perotitii* DC utilized in the current study were rinsed with sterile distilled water to eliminate any related dirt. The *M. perotitii* DC plant was air-dried for one week. The *M. perotitii* DC plant was ground using a pestle and mortar. The plan (20 g) was mixed in 100 ml of distilled water and ethanol in a ratio of 50:50, then incubated at room temperature for 24 hours [19]. Following the incubation period, the resulting infusion was properly filtered with Whatmann No. 1 filter paper and used for antibacterial tests.

C. *Qualitative Phytochemical Screening of* M. perotitii *DC Extract*

Qualitative phytochemical screening was performed to identify the presence of major secondary metabolites known to play crucial roles in nanoparticle biosynthesis. Five key phytochemical groups flavonoids, alkaloids, saponins, tannins, and phenolic compounds were specifically targeted because these biomolecules possess reducing and capping properties essential for green synthesis of metal oxide nanoparticles [20, 21]. Flavonoids and phenolic compounds contain hydroxyl groups that act as electron donors for metal ion reduction, while alkaloids, tannins, and saponins serve as stabilizing and capping agents that prevent excessive nanoparticle aggregation [10, 11]. These five classes represent the most bioactive constituents reported in *M. perotitii* and other Asteraceae family plants [16]. Standard qualitative tests were employed as described in previous phytochemical studies [20, 21].

TEST FOR FLAVONOIDS. (Alkaline Reagent Test) The extract (1 mL) was treated with 5 mL of NaOH. The presence of flavonoids was confirmed by the formation of the intense yellow color.

TEST FOR ALKALOIDS (Wagner's Test) The solvent extract (1 mL) was acidified with 1 mL of 1.5% v/v of HCl, and 1 mL of Wagner's reagent was added. The occurrence of alkaloids was indicated by the formation of yellow and/or brown precipitates.

TEST FOR SAPONINS (Frothing Test): About 1 mL of the extract was diluted separately with 20 mL of distilled water and was shaken in a graduated cylinder for 15 min. A 1 cm layer of foam was formed, which indicates the presence of saponins.

TEST FOR TANNINS AND PHENOLIC COMPOUNDS (ferric chloride test), the extract (1 mL) was treated with a few mL of 5% neutral ferric chloride. The formation of a dark blue and/or bluish-black colored product showed the presence of tannins and phenol.

D. *Preparation of NiO NPs using M. perotitii DC plant extract*

The synthesis procedure was adapted from the method previously described by [22]. Nickel (II) chloride

hexahydrate ($NiCl_2 \cdot 6H_2O$) served as the precursor. ($NiCl_2 \bullet 6H_2O$) (80 mL, 0.1 M) was measured and combined dropwise with 20 mL of the plant extract, *M. perotitii* DC, while being continuously stirred. After that, the mixture was heated to 80 degrees Celsius for two hours while being stirred with a magnetic stirrer. After allowing the mixture to cool to room temperature (25°C), it was centrifuged for 10 minutes at 10,000 rpm using a HERMLE Z326K centrifuge. The resultant pellet was rinsed three times with distilled water to get rid of contaminants after the supernatant was disposed of. After being cleaned, the pellet was placed in a Petri dish and dried in an oven set to 90°C. After drying, it was ground finely using a mortar and pestle, and any leftover organic material was then calcined for two hours at 500°C. For additional physicochemical characterization and biological assessments, the annealed NiO nanoparticle powder was ultimately stored in a tightly sealed glass vial.

E. *Antibacterial activities*

The antibacterial activity of the *Microtrichia perotitii* plant extract and the biosynthesized nickel oxide nanoparticles (NiO NPs) was assessed using a modified disc diffusion method [23–25]. The study was carried out against six bacterial strains comprising two Gram-positive bacteria *Staphylococcus aureus* (ATCC 33863) and *Bacillus subtilis* (ATCC 23857) and four Gram-negative bacteria *Pseudomonas aeruginosa* (ATCC 27853), *Salmonella typhi* (ATCC 19430), *Escherichia coli* (ATCC 25922), and *Clostridium botulinum* (ATCC 19397). All bacterial isolates were obtained from the Microbiology Laboratory of the University of Ilorin Teaching Hospital, Ilorin, Nigeria. The bacterial inoculum was prepared by adjusting freshly grown cultures to a turbidity equivalent to 10^8 CFU/mL (0.5 McFarland standard). A 100 µL aliquot of each suspension was evenly spread on the surface of sterile nutrient agar plates in three directions to ensure uniform growth. Sterile filter paper discs (6 mm in diameter) were impregnated with NiO NPs at different concentrations (25, 50, 75, and 100 µg/mL) and carefully placed on the inoculated agar surface. Discs containing *M. perotitii* plant extract (25 µg/mL) were also prepared to evaluate the antibacterial activity of the crude extract. Ciprofloxacin discs (5 µg) served as the positive control, while dimethyl sulfoxide (DMSO)-impregnated discs were used as the negative control to confirm that the solvent had no inhibitory effect. All inoculated plates were incubated at 37°C for 24 hours, after which the diameters of the inhibition zones were measured in millimeters using a digital Vernier caliper. The antibacterial potential of the NiO NPs and the plant extract was expressed as the mean ± standard deviation of triplicate determinations.

F. *Characterization*

The infrared spectrum of the solid NiO NPs was recorded using a Fourier-transform infrared (FTIR) spectrometer (ZN-FTIR 530, Shenzhen Zhuoneng Testing Technology Co., Ltd., Shenzhen, China) in the range of 4000-400 cm^{-1} using the KBr pellet technique to identify functional groups present in the nanoparticles. UV-Vis spectrophotometric analysis was performed using a SPECORD-200 spectrophotometer (Analytik Jena GmbH, Jena, Germany) in the wavelength range of 200-800 nm to analyze the optical properties of the nanoparticles. The morphology and particle shape of NiO NPs were examined using a scanning electron microscope (Phenom ProX model, Thermo Fisher Scientific, Eindhoven, Netherlands) operated at an accelerating voltage of 15 kV. The crystallographic structure was determined through X-ray diffraction using a Rigaku MiniFlex 600 XRD Diffractometer (Rigaku Corporation, Tokyo, Japan) with Cu Kα radiation ($\lambda = 1.5406$ Å) in the 2θ range of 10-80°. Additionally, the thermal stability of the nanoparticles was evaluated using a thermogravimetric analyzer (TGA-Q500 series, TA Instruments, New Castle, DE, USA) under a nitrogen atmosphere at a heating rate of 10°C/min from 30 to 900°C.

G. *Statistical Analysis*

The antibacterial assays was performed in triplicate, and the results are presented as mean ± standard deviation (SD). Statistical analysis was conducted using SPSS software (version 23, IBM Corporation, Armonk, NY, USA). A two-way analysis of variance (ANOVA) was employed, and differences were considered statistically significant at a p-value of less than 0.05.

III. RESULTS

A. *Phytochemical screening of M. perotitii DC*

Evaluation of *M. perotitii*'s ethanolic leaf extract using phytochemistry. The phytochemical test used to support the different kinds of bioactive compounds present in the plant extract of *M. perotitii* is shown in Table 1. The synthesis of molecules with specific functions benefits from an understanding of the connection between phytoconstituents and plant bioactivity. A straightforward decoction process with ethanol was used to create the *M. perotitii* plant extract. The result was a green extract. The most significant bioactive components of the plant are compiled in Table 1. This result is quite consistent with previous research. [20, 21]

Table 1: Qualitative phytochemical screening of *M. perotitii* DC plant extract

S/N	Phytochemical	Test	Results
1	Alkaloids	Wagner	+
2	Tannins	Ferric Chloride	+
3	Saponins	Frothing	+
4	Phenolics	Ferric Chloride	+
5	Flavonoids	Alkaline	+

B. *Fourier transforms infrared spectroscopy (FTIR) studies*

The FTIR spectrum of nickel oxide nanoparticles (NiO NPs) made with leaf extract from *Microtrichia perotitii* DC is shown in Figure 1. To determine the functional groups and validate the formation of NiO NPs, the spectra were captured using the KBr pellet technique in the 4000–400 cm^{-1} range. Because of metal–oxygen lattice vibrations, metal oxide absorption and transmission bands usually occur in the 400–1500 cm^{-1} range [26]. The O–H stretching vibrations of hydroxyl groups, which may be derived from phenolic compounds and adsorbed water molecules, are represented by a broad peak seen at 3372 cm^{-1} [18, 26]. The C=O stretching vibration of carbonyl groups was responsible for the absorption band at 1671 cm^{-1}, whereas the C–H and C–O stretching vibrations are linked to the peaks at 2971 cm^{-1} and 1068 cm^{-1}, respectively. Furthermore, residual biomolecules in the plant extract may be responsible for the band at 856 cm^{-1} through phenolic ring vibrations or C–H bending. Crucially, the successful formation of NiO nanoparticles is confirmed by the clear absorption band seen at 651 cm^{-1}, which correlates to Ni–O stretching vibrations. This result is in line with earlier reports on green-synthesized NiO NPs' FTIR spectra [17].

The spectra's presence of both organic (O–H, C=O, C–H, and C–O) and inorganic (Ni–O) functional groups indicates that the *M. perotitii* extract's phytochemicals, including flavonoids, phenols, and other oxygenated compounds, took part in the bioreduction of Ni^{2+} ions before acting as stabilizing and capping agents. Consequently, the FTIR analysis not only validates the formation of NiO but also offers proof of the reduction and surface stabilization mechanisms aided by phytochemicals [27].

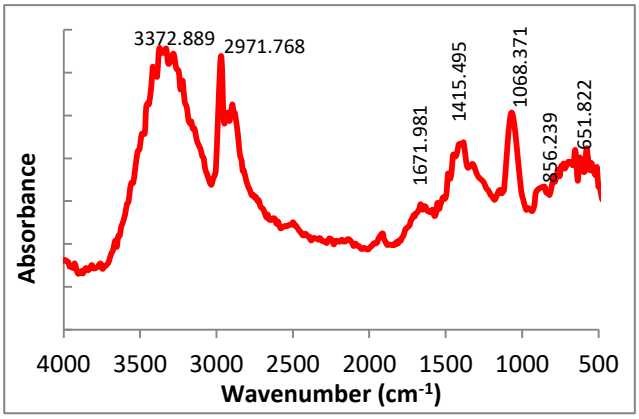

Figure 1: FTIR spectrum of *M. perotitii* synthesized NiO NPs

C. *Optical properties of NiO NPs*

The UV-visible (UV-Vis) absorption spectrum of nickel oxide nanoparticles (NiO NPs) made with leaf extract from *Microtrichia perotitii* DC is shown in Figure 2. The intrinsic electronic transition of NiO, which corresponds to the charge transfer between O^{2-} and Ni^{2+} ions, is responsible for the absorption band seen at about 365 nm [28]. This absorption feature, which is within the typical range (320–380 nm) reported for biosynthesized NiO NPs, validates the successful formation of NiO nanoparticles [29]. At longer wavelengths, there is less photon interaction, indicating uniform particle distribution and aggregation, as indicated by a progressive decrease in absorbance intensity with increasing wavelength. The presence of tiny, evenly distributed nanoparticles with a narrow size distribution is further suggested by the sharp absorption edge.

Depending on the synthesis conditions and particle size, the band gap energy (Eg) of NiO, which normally ranges between 3.4 and 4.0 eV for nanoscale NiO [30], can also be linked to the optical absorption edge at 365 nm. The formation of nanosized particles is further supported by quantum confinement effects, which are indicated by the slight blue shift in the absorption band (~380 nm) compared to bulk NiO. These findings validate that *M. perotitii* DC extract successfully promoted the reduction and stabilization of nickel ions during

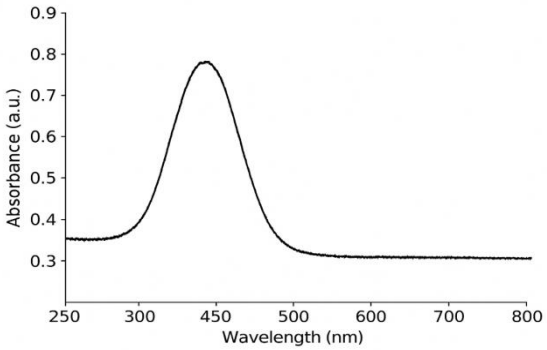

nanoparticle formation, as they are consistent with earlier research on green-synthesized NiO NPs.

Figure 2: Absorption spectrum of *M. perotitii* synthesized NiO NPs

D. *X-ray diffractometry (XRD) analysis*

The crystallinity and phase structure of the biosynthesized nickel oxide nanoparticles (NiO NPs) were assessed using X-ray diffraction (XRD) analysis. The XRD diffraction pattern of NiO NPs made with leaf extract from *Microtrichia perotitii* DC is shown in Figure 3. Significant diffraction peaks were detected at 2θ = 37.3°, 43.8°, 63.5°, 75.3°, and 79.4°, corresponding to the crystal planes (111), (200), (220), (311), and (222), respectively. These planes support the formation of pure crystalline NiO since they are consistent with the standard cubic (bunsenite) phase of NiO as identified by JCPDS card no. 00-025-1044. High phase purity and a successful conversion of the precursor into NiO nanoparticles during synthesis were indicated by the absence of any additional peaks associated with impurities. The Debye-Scherrer equation was used to determine the average crystallite size (D).

$$D = \frac{K\lambda}{\beta \cos\theta} \qquad (1)$$

Where λ is the X-ray wavelength (1.5406 Å for Cu Kα radiation), β is the full width at half maximum (FWHM) of the diffraction peak (in radians), θ is the Bragg angle, D is the average crystallite size, and K is the shape factor (0.89). The synthesized NiO NPs were found to have an average crystallite size calculated using the Scherrer equation of24 nm, which is within the usual range for green-synthesized NiO nanoparticles [13]. High levels of crystallinity are indicated by the comparatively sharp and intense diffraction peaks, whereas the presence of nanocrystalline domains is suggested by a slight broadening of the peaks. A number of variables, including the synthesis conditions, calcination temperature, and plant extract concentration, can affect the observed crystallite size and peak sharpness [6, 31]. The findings demonstrated that the phytochemicals

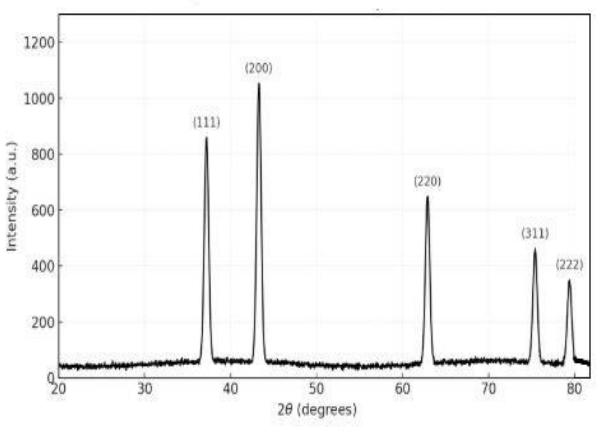

Figure 3: XRD pattern of *M. perotitii* synthesized NiO NPs

E. *Surface morphology characterization*

Scanning electron microscopy (SEM) was used to analyze the surface morphology of the biosynthesized nickel oxide nanoparticles (NiO NPs). Figure 4 displayed the corresponding micrographs taken at 1000× magnification. According to the images, the NiO NPs were densely distributed, irregularly shaped, and showed clear signs of agglomeration, forming clusters of different sizes. The strong van der Waals interactions, magnetic attractions, and high surface energy characteristic of nanosized particles are responsible for this aggregation, which is frequently seen in green-synthesized metal oxides [6]. A polycrystalline nature, where smaller crystallites combine to form larger aggregates, is suggested by the microstructural appearance. The partial covering of phytochemical residues from the *M. perotitii* extract may be the cause of the particle surfaces' rough and granular textures. During synthesis, these biomolecules most likely served as stabilizing and capping agents, affecting the nucleation and development of the nanoparticles. For catalytic, electrochemical, and adsorption-based applications, the significant agglomeration and granular morphology also suggested a large specific surface area [13, 32]. The green-synthesized NiO NPs have nanocrystalline, poly-agglomerated structures stabilized by organic constituents from the plant extract, as confirmed by the overall SEM observations and XRD results.

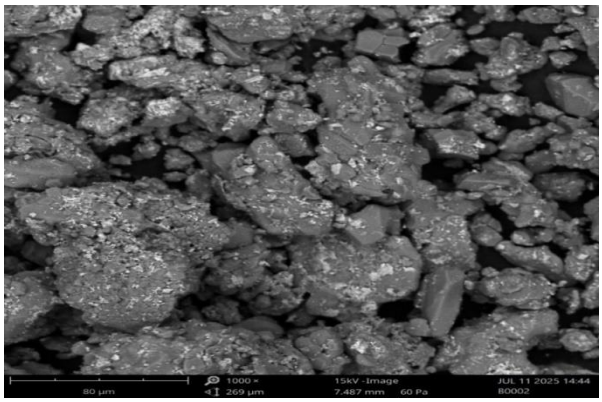

Figure 4: SEM micrograph *M. perotitii* synthesized NiO NPs at different magnification

F. *Thermogravimetry/Differential Thermal Analysis (TG/DTA)*

Thermogravimetric analysis (TGA) and differential thermal analysis (DTA) were used to investigate the thermal stability and compositional behavior of the biosynthesized nickel oxide nanoparticles (NiO NPs), as illustrated in Figure 5. Over a temperature range of 30 to 900°C, the analysis was carried out in a nitrogen atmosphere at a heating rate of 10°C/min. Multiple stages of overall weight loss resulted in a final residue of roughly 19.6% at 900°C, which is equivalent to the thermally stable NiO phase. The evaporation of adsorbed moisture and the elimination of volatile surface-bound species are responsible for the initial slight weight loss of roughly 4% in the 50–220°C range [17]. The thermal breakdown of remaining phytochemical compounds from the *M. perotitii* extract is linked to the second stage of weight loss, which occurs at 262°C and is about 14.2%. During the synthesis of nanoparticles, these organic moieties served as capping and reducing agents and are normally removed at moderate temperatures [33]. At about 473°C, a significant weight loss of 61.2% was noted, which is consistent with the crystallization of the NiO lattice structure and the oxidative degradation of the residual organic residues. No discernible mass loss was seen above 500°C, suggesting that the material underwent full conversion to thermally stable NiO. The DTG curve showed clear endothermic peaks at temperatures of about 300°C and 450°C, which stand for the organic constituents' maximum rates of degradation. All things considered, the TGA/DTA results showed that the biosynthesized NiO NPs have outstanding thermal stability above 500°C, proving their structural soundness and appropriateness for high-temperature uses like energy storage, gas sensing, and catalysis.

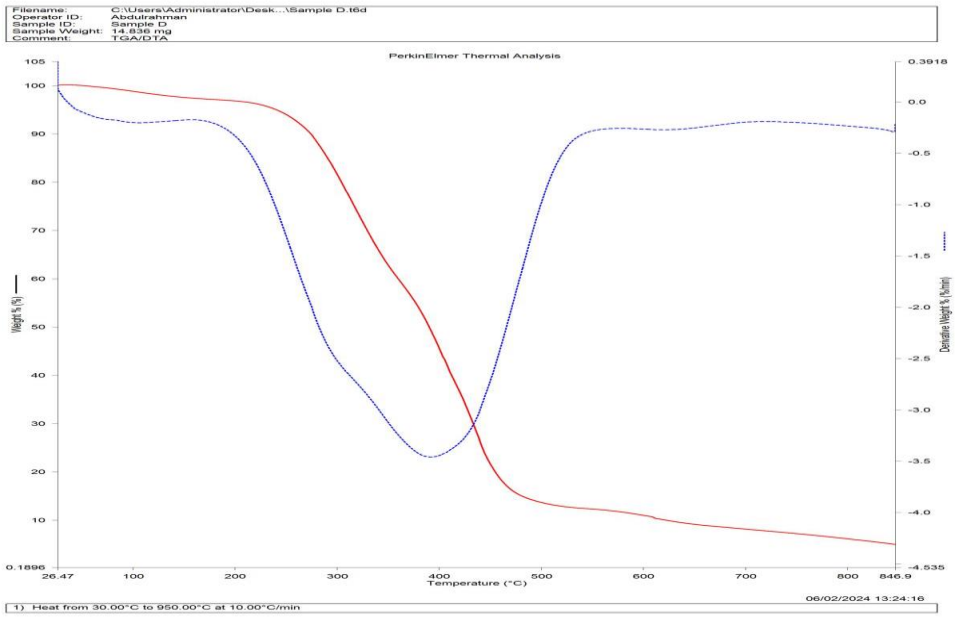

Figure 5: TGA-DTA curve of *M. perotitii* synthesized NiO NPs.

G. *Evaluation of antibacterial activity using NiO NPs prepared using M. perotitii DC plant extract*

Two Gram-positive species, *Staphylococcus aureus* (ATCC 33863) and *Bacillus subtilis* (ATCC 23857), and four Gram-negative species, *Pseudomonas aeruginosa* (ATCC 27853), *Salmonella typhi* (ATCC 19430), *Escherichia coli* (ATCC 25922), and *Clostridium botulinum* (ATCC 19397), were used to test the antibacterial activity of the *Microtrichia perotitii* DC leaf extract and its biosynthesized nickel oxide nanoparticles (NiO NPs). NiO NP concentrations of 25, 50, 75, and 100 µg/mL were used in the antibacterial evaluation, which was carried out using the agar well diffusion method.

The green-synthesized NiO NPs' antibacterial activity was concentration-dependent, as indicated in Table 2, with the inhibition zones gradually growing as the nanoparticle concentration rose. Across all tested microorganisms, the NiO NPs demonstrated greater antibacterial activity than the crude *M. perotitii* extract, even at the lowest concentration (25 µg/mL). The inhibition zones for S. aureus and E. coli at this concentration were 11.4 ± 0.5 mm and 8.1 ± 0.3 mm, respectively. Higher concentrations showed a significant increase in antibacterial activity; at 100 µg/mL, *S. aureus* and *B. subtilis* showed inhibition zones of 19.6 ± 0.4 mm and 18.8 ± 0.6 mm, respectively. Of the Gram-negative isolates, E. coli (13.2 ± 0.4 mm) and *P. aeruginosa* 12.8 ± 0.6 mm) showed moderate sensitivity, while S. typhi (15.9 ± 0.3 mm) showed the highest susceptibility, followed by *C. botulinum* (14.7 ± 0.5 mm).

The NiO NPs showed exceptional antibacterial potency, especially against Gram-positive bacteria, even though the standard antibiotic ciprofloxacin produced slightly larger inhibition zones (ranging from 18.5 ± 0.3 mm to 23.1 ± 0.4 mm). The synergistic influence of phytochemicals, particularly flavonoids, polyphenols, and terpenoids, which function as capping agents, increase surface reactivity, and encourage the production of reactive oxygen species (ROS), which causes oxidative stress, cell membrane disruption, and protein denaturation in bacterial cells, was responsible for the higher activity of the NiO NPs made with *M. perotitii* extract [34, 35]. Gram-negative bacteria are known to have comparatively smaller inhibition zones because of their intricate cell wall architecture, which includes a thinner peptidoglycan layer and an outer membrane rich in lipopolysaccharides. This structure limits the ionic interaction between Ni^{2+} ions and the cell surface and prevents nanoparticle penetration. Their superior resistance to Gram-positive bacteria is a result of this barrier, which also offers extra protection. These findings are in line with earlier research that found that Gram-negative bacteria's effective efflux mechanisms and outer membrane impermeability contribute to their increased resistance to metal oxide nanoparticles and traditional antibiotics [35–41].

All together, these results validate the potential use of *M. perotitii-mediated* NiO NPs in antimicrobial coatings, wound dressings, and biomedical formulations by confirming that they have broad-spectrum antibacterial qualities with stronger inhibition against Gram-positive bacteria.

Table 2: Antimicrobial activity of *M. perotitii* synthesized NiO NPs

Pathogenic Bacteria	Diameter of Inhibition Zone (mm)				Positive control Ciprofloxacin (5 µg disk)	plant Extract (25 µg mL^{-1})
	NiO NPs					
	25 µg mL^{-1}	50 µg mL^{-1}	75 µg mL^{-1}	100 µg mL^{-1}		
S. aureus	11.4±0.50^{a}	13.8±0.70^{b}	15.7±0.30^{f}	19.6±0.40^{d}	23.1 ± 0.43^{c}	9.1 ± 0.32^{e}
B. subtilis	10.9±0.30^{c}	12.7±0.51^{e}	14.9±0.40^{b}	18.8±0.60^{c}	22.4± 0.50^{a}	8.3 ± 0.23^{d}
P. aeruginosa	8.4 ± 0.31^{d}	10.2±0.53^{f}	11.6 ± 1.0^{a}	12.8±0.60^{b}	19.6 ± 0.35^{e}	6.8 ± 0.70^{g}
S. typhi	9.2±0.40^{e}	11.4±0.30^{c}	13.5±0.42^{f}	15.9±0.38^{d}	21.7±0.40^{a}	7.5±0.53^{b}
E. coli	8.1±0.30^{a}	10.6±0.5^{d}	11.8±0.60^{e}	13.2±0.70^{c}	20.5±0.62^{b}	7.2±0.80^{f}
C. botulinum	9.7 ± 0.50^{f}	11.8±0.14^{b}	13.2 ± 1.1^{c}	14.7±0.80^{e}	18.5 ± 0.30^{a}	8.6 ± 0.25^{d}

The superscript lettered (a-f) indicate significant difference (at $p < 0.05$) when subject to SPSS test. The findings are given as mean ± standard deviation

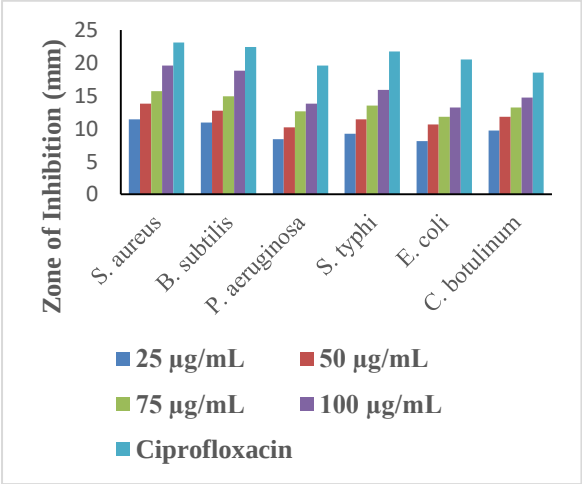

Figure 6: Antimicrobial activity of *M. perotitii* synthesized NiO

IV. DISCUSSION

The green synthesis of NiO nanoparticles using leaf extract from *Microtrichia perotitii* DC shows how the plant's various phytochemicals all work together to promote the formation, stabilization, and functionality of nanoparticles. By donating electrons from hydroxyl groups to change Ni^{2+} into Ni^{0}, which then formed NiO during calcination at 500°C, flavonoids, phenolics, tannins, alkaloids, and saponins acted as reducing and capping agents [42]. During the synthesis of nanoparticles, functional groups like hydroxyl and carboxyl groups actively participate as reducing agents, and plant metabolites are known to scavenge free radicals [43]. Thus, the presence of these metabolites, particularly alkaloids, saponins, flavonoids, phenolics, and tannins, suggests that the extract contains a significant amount of bioactive reducing agents [16, 33].

The participation of these phytochemicals was validated by FTIR analysis, which revealed distinctive Ni–O stretching at 651 cm^{-1} in addition to O–H, C=O, and C–O vibrations from leftover organic compounds. By forming an organic shell around the NiO core, these surface-bound biomolecules establish a direct connection between the synthesis mechanism and the stabilization of the nanoparticles and their subsequent functional behavior. Agglomerated clusters with irregular shapes and dense packing were found by SEM analysis. Van der Waals forces, which pull particles together, cause this kind of agglomeration to occur frequently in nanoparticles with small particle sizes [43, 44]. The intrinsically high surface energy and surface tension of NiO at the nanoscale are also responsible for this behavior, according to earlier research [44, 46].

The reported morphological differences between NiO NPs made with Arabic gum [47] and *Spirostachys africana* [46] highlight the fact that particle size and shape are greatly influenced by the kind and concentration of phytochemicals found in each plant extract. The structural properties of the nanoparticles also show the influence of the phytochemical composition. In line with findings on other plant-mediated NiO nanoparticles [13, 31], XRD analysis revealed a pure cubic bunsenite phase with an average crystallite size of 24 nm. Nanoparticle crystallinity is known to be impacted by variations in size, shape, and precursor chemistry, which can result in variations in XRD peak intensity.

The capping activity of polyphenols from *M. perotitii*, which restricts unchecked particle growth, may be responsible for the very small crystallite size obtained in this investigation. The UV–Vis spectrum, which showed a strong absorption peak at 365 nm, corresponding to the NiO band gap (3.4–4.0 eV), supports this homogeneity. The absorption peak further demonstrates the stability and good dispersion of the produced NiO NPs. The combined effects of the manufacturing process and the phytochemical coating were shown by thermal analysis (TGA/DTA). Thermally stable NiO was left at 500°C as a result of the breakdown of loosely and tightly bound organic residues, whereas the initial mass loss was attributed to desorbed water [17].

The substantial organic content before calcination indicates considerable biomolecule interaction with the nickel precursor, which contributed to regulated nucleation, stability, and the development of a protective organic shell. This intimate link between phytochemical-mediated synthesis and structural-morphological characteristics naturally extends to the nanoparticles' thermal properties [47, 48]. The antibacterial activity demonstrates how synthesis, structure, morphology, and temperature behavior all influence functional performance. The small crystallite size, controlled by phytochemicals, allowed for close interaction with bacterial membranes, while the organic shell provided extra antibacterial activity. NiO nanoparticles produce ROS and release Ni^{2+} ions, causing oxidative stress, membrane damage, and DNA breakage in bacterial cells [34-36].

The increased susceptibility of Gram-positive bacteria in this study is consistent with their accessible peptidoglycan layer, and it supports the combined effects of particle size, surface chemistry, and NiO's inherent antibacterial pathways [39, 40]. Overall, the synergistic interplay of the inorganic NiO core and organic phytochemical coating demonstrates that the synthesis mechanism provides the foundation for all subsequent structural, optical, thermal, morphological, and biological aspects. Using *Microtrichia perotitii* DC extract provides a sustainable and effective method for manufacturing NiO nanoparticles with regulated size, crystallinity, shape, and increased antibacterial activity.

IV. CONCLUSION

This study successfully demonstrates the potential of *Microtrichia perotitii* DC leaf extract as an efficient, sustainable, and bioactive source for the green synthesis of nickel oxide nanoparticles (NiO NPs). The extract's diverse phytochemical composition, rich in alkaloids, flavonoids, and phenolic compounds, acted synergistically as both reducing and capping agents, facilitating the formation of stable nanocrystalline NiO. Spectroscopic and microscopic analyses confirmed the successful synthesis. FTIR verified the presence of Ni–O bonds and residual organic moieties; XRD revealed well-defined crystalline nanoparticles with an average crystallite size of approximately 24 nm; UV–Vis spectroscopy showed a distinct surface plasmon resonance band; and SEM images displayed irregular, agglomerated morphologies typical of plant-mediated synthesis. The biosynthesized NiO NPs exhibited pronounced antibacterial activity, particularly against Gram-positive strains such as *Bacillus subtilis* and *Staphylococcus aureus*, with inhibition zones reaching 19.6 ± 0.40 mm at 100 μg mL^{-1}, slightly lower but comparable to ciprofloxacin (5 μg/disc). The lower sensitivity observed in Gram-negative bacteria likely results from their outer membrane barrier, which restricts nanoparticle penetration. These findings suggest that the antimicrobial efficacy arises from the combined effects of the NiO nanostructure and the phytochemical residues adsorbed on its surface. Overall, this work establishes *M. perotitii* DC as a novel biogenic agent for eco-friendly NiO NP synthesis and underscores the influence of plant extract composition on nanoparticle bioactivity. The promising antibacterial performance supports further studies aimed at elucidating the mechanistic pathways of microbial inhibition, optimizing synthesis parameters for controlled particle size and dispersion, and exploring broader biomedical and environmental applications.

CONFLICT OF INTEREST

Authors declare that they have no conflict of interest.

V. REFERENCES

[1] I. Fatimah *et al.*, "Synthesis and control of the morphology of SnO2 nanoparticles via various concentrations of Tinospora cordifolia stem extract and reduction methods," *Arabian Journal of Chemistry*, vol. 15, no. 4, p. 103738, Feb. 2022, doi: 10.1016/j.arabjc.2022.103738.

[2] N.-D. Jaji, H. L. Lee, M. H. Hussin, H. M. Akil, M. R. Zakaria, and M. B. H. Othman, "Advanced nickel nanoparticles technology: From synthesis to applications," *Nanotechnology Reviews*, vol. 9, no. 1, pp. 1456–1480, Jan. 2020, doi: 10.1515/ntrev-2020-0109.

[3] F. L. Jia, L. Z. Zhang, X. Y. Shang, and Y. Yang, "Non-Aqueous Sol–Gel Approach towards the Controllable Synthesis of Nickel Nanospheres, Nanowires, and Nanoflowers," *Advanced Materials*, vol. 20, no. 5, pp. 1050–1054, Feb. 2008, doi: 10.1002/adma.200702159.

[4] A. Kar, "Synthesis of Nano-Spherical nickel by templating hibiscus flower petals," *American Journal of Nanoscience and Nanotechnology*, vol. 2, no. 2, p. 17, Jan. 2014, doi: 10.11648/j.nano.20140202.11.

[5] P. Laokul, V. Amornkitbamrung, S. Seraphin, and S. Maensiri, "Characterization and magnetic properties of nanocrystalline CuFe2O4, NiFe2O4, ZnFe2O4 powders prepared by the Aloe vera extract solution," *Current Applied Physics*, vol. 11, no. 1, pp. 101–108, Jul. 2010, doi: 10.1016/j.cap.2010.06.027.

[6] R. Lefojane *et al.*, "Green Synthesis of Nickel Oxide (NiO) Nanoparticles Using Spirostachys africana Bark Extract," *Asian Journal of Scientific Research*, vol. 13, no. 4, pp. 284–291, Sep. 2020, doi: 10.3923/ajsr.2020.284.291.

[7] J. Moavi, F. Buazar, and M. H. Sayahi, "Algal magnetic nickel oxide nanocatalyst in accelerated

synthesis of pyridopyrimidine derivatives," *Scientific Reports*, vol. 11, no. 1, p. 6296, Mar. 2021, doi: 10.1038/s41598-021-85832-z.

[8] A. Mueez, S. Hussain, M. Ahmad, A. Raza, I. Ahmed, and M. Amjad, "GREEN SYNTHESIS OF NANOSILVER PARTICLES FROM PLANTS EXTRACT," *International Journal of Agriculture Environment and Bioresearch*, vol. 07, no. 01, pp. 96–122, Jan. 2022, doi: 10.35410/ijaeb.2022.5703.

[9] N. S. Nosheen *et al.*, "A review: Development of magnetic nano vectors for biomedical applications," *GSC Advanced Research and Reviews*, vol. 8, no. 2, pp. 085–110, Aug. 2021, doi: 10.30574/gscarr.2021.8.2.0169.

[10] M. A. Rahman, R. Radhakrishnan, and R. Gopalakrishnan, "Structural, optical, magnetic and antibacterial properties of Nd doped NiO nanoparticles prepared by co-precipitation method," *Journal of Alloys and Compounds*, vol. 742, pp. 421–429, Jan. 2018, doi: 10.1016/j.jallcom.2018.01.298.

[11] L. M. Rossi, A. D. Quach, and Z. Rosenzweig, "Glucose oxidase?magnetite nanoparticle bioconjugate for glucose sensing," *Analytical and Bioanalytical Chemistry*, vol. 380, no. 4, pp. 606–613, Sep. 2004, doi: 10.1007/s00216-004-2770-3.

[12] S. S. Sana *et al.*, "Biogenesis and Application of nickel nanoparticles: A review," *Current Pharmaceutical Biotechnology*, vol. 22, no. 6, pp. 808–822, Jan. 2021, doi: 10.2174/1389201022999210101235233.

[13] H. Shabbir and A. Muhammad, "A Review on Gold Nanoparticles (GNPs) and their Advancement in Cancer Therapy," *International Journal of Nanomaterials Nanotechnology and Nanomedicine*, pp. 019–025, Jan. 2021, doi: 10.17352/2455-3492.000040.

[14] M. Shah, D. Fawcett, S. Sharma, S. Tripathy, and G. Poinern, "Green synthesis of metallic nanoparticles via biological entities," *Materials*, vol. 8, no. 11, pp. 7278–7308, Oct. 2015, doi: 10.3390/ma8115377.

[15] S. Suresh *et al.*, "Star fruit extract-mediated green synthesis of metal oxide nanoparticles," *Inorganic and Nano-Metal Chemistry*, vol. 52, no. 2, pp. 173–180, Feb. 2021, doi: 10.1080/24701556.2021.1880437.

[16] M. Abdullahi, "Phytochemical Screening and Biological Studies of the Leaves of Microtrichia perotitii DC (Asteraceae)," *European Journal of Medicinal Plants*, vol. 1, no. 3, pp. 88–97, Jan. 2011, doi: 10.9734/ejmp/2011/188.

[17] S. Hussain *et al.*, "Green synthesis of nickel oxide nanoparticles using Acacia nilotica leaf extracts and investigation of their electrochemical and biological properties," *Journal of Taibah University for Science*, vol. 17, no. 1, Feb. 2023, doi: 10.1080/16583655.2023.2170162.

[18] A. Habtemariam and M. Oumer, "Plant extract mediated synthesis of nickel oxide nanoparticles," *Materials International*, vol. 2, no. 2, pp. 205–209, Apr. 2020, doi: 10.33263/materials22.205209.

[19] A. A. Ezhilarasi, J. J. Vijaya, K. Kaviyarasu, M. Maaza, A. Ayeshamariam, and L. J. Kennedy, "Green synthesis of NiO nanoparticles using Moringa oleifera extract and their biomedical applications: Cytotoxicity effect of nanoparticles against HT-29 cancer cells," *Journal of Photochemistry and Photobiology B Biology*, vol. 164, pp. 352–360, Oct. 2016, doi: 10.1016/j.jphotobiol.2016.10.003.

[20] H. Gebreslassie and A. Eyasu, "Phytochemical screening of the leaves Calpurnia aurea (Ait.) benth extract," *International Journal of Clinical Chemistry and Laboratory Medicine*, vol. 5, no. 4, Jan. 2019, doi: 10.20431/2455-7153.0504004.

[21] K. Ganesan, S. Kumar, P. Nair, N. Letha, and G. Banu, *Phytochemical Screening of Different Solvent Extracts of Soap Berry (Phytolacca dodecandra L' Herit.) - A Native Ethiopian Shrub*, 2016.

[22] A. A. Ezhilarasi, J. J. Vijaya, K. Kaviyarasu, M. Maaza, A. Ayeshamariam, and L. J. Kennedy, "Green synthesis of NiO nanoparticles using Moringa oleifera extract and their biomedical applications: Cytotoxicity effect of nanoparticles against HT-29 cancer cells," *Journal of Photochemistry and Photobiology B Biology*, vol. 164, pp. 352–360, Oct. 2016, doi: 10.1016/j.jphotobiol.2016.10.003.

[23] S. T. B. Kazmi *et al.*, "Phytochemical analysis and comprehensive evaluation of pharmacological potential of Artemisia brevifolia Wall. ex DC," *Saudi Pharmaceutical Journal*, vol. 30, no. 6, pp. 793–814, Mar. 2022, doi: 10.1016/j.jsps.2022.03.012.

[24] I. A. Mohammed, M. Ahmed, R. Ikram, M. Muddassar, M. A. Qadir, and K. B. Awang, "Synthesis of 1,3-benzoxazines based on 2,4,4-trimethyl-7,2',4'-trihydroxy flavan: antibacterial, anti-inflammatory, cyclooxygenase-2 inhibition and molecular modelling studies," *Letters in Drug Design & Discovery*, vol. 16, no. 1, pp. 58–65, Apr. 2018, doi: 10.2174/1570180815666180420100922.

[25] S. Ahmed, N. Saifullah, M. Ahmad, B. L. Swami, and S. Ikram, "Green synthesis of silver nanoparticles using Azadirachta indica aqueous leaf extract," *Journal of Radiation Research and Applied Sciences*, vol. 9, no. 1, pp. 1–7, Jun. 2015, doi: 10.1016/j.jrras.2015.06.006.

[26] H. Kumar and R. Rani, "Structural and optical characterization of ZNO nanoparticles synthesized by microemulsion route," *International Letters of Chemistry Physics and Astronomy*, vol. 19, pp. 26–36, Oct. 2013, doi: 10.18052/www.scipress.com/ilcpa.19.26

[27] M. Alagiri, S. Ponnusamy, and C. Muthamizhchelvan, "Synthesis and characterization of NiO nanoparticles by sol–gel method," *Journal of Materials Science Materials in Electronics*, vol. 23, no. 3, pp. 728–732, Aug. 2011, doi: 10.1007/s10854-011-0479-6.

[28] S. G. Firisa, G. G. Muleta, and A. A. Yimer, "Synthesis of Nickel Oxide Nanoparticles and Copper-Doped Nickel Oxide Nanocomposites Using Phytolacca dodecandra L'Herit Leaf Extract and Evaluation of Its Antioxidant and Photocatalytic Activities," *ACS Omega*, vol. 7, no. 49, pp. 44720–44732, Dec. 2022, doi: 10.1021/acsomega.2c04042.

[29] M. Ramesh, "N and Fe doped NiO nanoparticles for enhanced photocatalytic degradation of azo dye methylene blue in the presence of visible light," *SN Applied Sciences*, vol. 3, no. 10, Sep. 2021, doi: 10.1007/s42452-021-04803-1.

[30] S. J. Musevi, A. Aslani, H. Motahari, and H. Salimi, "Offer a novel method for size appraise of NiO nanoparticles by PL analysis: Synthesis by sonochemical method," *Journal of Saudi Chemical Society*, vol. 20, no. 3, pp. 245–252, Jul. 2012, doi: 10.1016/j.jscs.2012.06.009.

[31] R. Lefojane *et al.*, "Green Synthesis of Nickel Oxide (NiO) Nanoparticles Using Spirostachys africana Bark Extract," *Asian Journal of Scientific Research*, vol. 13, no. 4, pp. 284–291, Sep. 2020, doi: 10.3923/ajsr.2020.284.291.

[32] S. U. R *et al.*, "Biogenic Synthesis of NiO Nanoparticles Using Areca catechu Leaf Extract and Their Antidiabetic and Cytotoxic Effects," *Molecules*, vol. 26, no. 9, p. 2448, Apr. 2021, doi: 10.3390/molecules26092448.

[33] M. Sepahvand, F. Buazar, and M. H. Sayahi, "Novel marine-based gold nanocatalyst in solvent-free synthesis of polyhydroquinoline derivatives: Green and sustainable protocol," *Applied Organometallic Chemistry*, vol. 34, no. 12, Sep. 2020, doi: 10.1002/aoc.6000.

[34] G. Basak, D. Das, and N. Das, "Dual Role of Acidic Diacetate Sophorolipid as Biostabilizer for ZnO Nanoparticle Synthesis and Biofunctionalizing Agent Against Salmonella enterica and Candida albicans," *Journal of Microbiology and Biotechnology*, vol. 24, no. 1, pp. 87–96, Jan. 2014, doi: 10.4014/jmb.1307.07081.

[35] I. Fatimah, R. Y. Pradita, and A. Nurfalinda, "Plant extract mediated of ZNO nanoparticles by using ethanol extract of mimosa pudica leaves and coffee powder," *Procedia Engineering*, vol. 148, pp. 43–48, Jan. 2016, doi: 10.1016/j.proeng.2016.06.483.

[36] Bindhu and M. Umadevi, "Antibacterial activities of green synthesized gold nanoparticles," *Materials Letters*, vol. 120, pp. 122–125, Jan. 2014, doi: 10.1016/j.matlet.2014.01.108.

[37] T. Muthukumar, N. Sudhakumari, B. Sambandam, A. Aravinthan, T. P. Sastry, and J.-H. Kim, "Green synthesis of gold nanoparticles and their enhanced synergistic antitumor activity using HepG2 and MCF7 cells and its antibacterial effects," *Process Biochemistry*, vol. 51, no. 3, pp. 384–391, Jan. 2016, doi: 10.1016/j.procbio.2015.12.017.

[38] H. K. Allen, J. Donato, H. H. Wang, K. A. Cloud-Hansen, J. Davies, and J. Handelsman, "Call of the wild: antibiotic resistance genes in natural environments," *Nature Reviews Microbiology*, vol. 8, no. 4, pp. 251–259, Mar. 2010, doi: 10.1038/nrmicro2312.

[39] J. a. H. Romaniuk and L. Cegelski, "Bacterial cell wall composition and the influence of antibiotics by cell-wall and whole-cell NMR," *Philosophical Transactions of the Royal Society B Biological Sciences*, vol. 370, no. 1679, p. 20150024, Sep. 2015, doi: 10.1098/rstb.2015.0024.

[40] D. a. C. Heesterbeek *et al.*, "Publisher Correction: Complement-dependent outer membrane perturbation sensitizes Gram-negative bacteria to Gram-positive specific antibiotics," *Scientific Reports*, vol. 9, no. 1, p. 7841, May 2019, doi: 10.1038/s41598-019-43208-4.

[41] J. Davies and D. Davies, "Origins and evolution of antibiotic resistance," *Microbiology and Molecular Biology Reviews*, vol. 74, no. 3, pp. 417–433, Aug. 2010, doi: 10.1128/mmbr.00016-10.

[42] J. Sukumaran, M. Priya, R. Venkatesan, K. Sathiasivan, M. R. Khan, and S. Kim, "Green Synthesis of Nickel Oxide Nanoparticles Using Leaf Extract of Aegle marmelos and Their Antibacterial, Anti-Oxidant, and In Vitro Cytotoxicity Activity," *Microscopy Research and Technique*, vol. 88, no. 10, pp. 2830–2842, Jul. 2025, doi: 10.1002/jemt.70054.

[43] A. Kanchana, S. Devarajan, and S. R. Ayyappan, "Green synthesis and characterization of palladium nanoparticles and its conjugates from solanum trilobatum leaf extract," *Nano-Micro Letters*, vol. 2, no. 3, pp. 169–176, Sep. 2010, doi: 10.1007/bf03353637.

[44] R. Lefojane *et al.*, "Green Synthesis of Nickel Oxide (NiO) Nanoparticles Using Spirostachys africana Bark Extract," *Asian Journal of Scientific Research*, vol. 13, no. 4, pp. 284–291, Sep. 2020, doi: 10.3923/ajsr.2020.284.291.

[45] B. J. Landi, H. J. Ruf, C. M. Evans, C. D. Cress, and R. P. Raffaelle, "Purity assessment of Single-Wall carbon nanotubes, using optical absorption spectroscopy," *The Journal of Physical Chemistry B*, vol. 109, no. 20, pp. 9952–9965, Apr. 2005, doi: 10.1021/jp044990c.

[46] S. T. Fardood, A. Ramazani, and S. Moradi, "A novel green synthesis of nickel oxide nanoparticles using arabic gum," *Chemistry Journal of Moldova*, vol. 12, no. 1, pp. 115–118, May 2017, doi: 10.19261/cjm.2017.383.

[47] V. Biju and M. A. Khadar, "Electronic structure of nanostructured nickel oxide using NI 2P XPS analysis," *Journal of Nanoparticle Research*, vol. 4, no. 3, pp. 247–253, Jun. 2002, doi: 10.1023/a:1019949805751.

[48] S. Farooq, M. Habib, O. Cardozo, K. Ullah, A. K. Pandey, and Z. Said, "Exploring the impact of particle stability, size, and morphology on nanofluid thermal conductivity: A comprehensive review for energy applications," *Advances in Colloid and Interface Science*, vol. 341, p. 103495, Mar. 2025, doi: 10.1016/j.cis.2025.103495.

[49] K. Deka *et al.*, "Understanding the mechanism underlying the green synthesis of metallic nanoparticles using plant extract(s) with special reference to Silver, Gold, Copper and Zinc oxide nanoparticles," *Hybrid Advances*, vol. 9, p. 100399, Feb. 2025, doi: 10.1016/j.hybadv.2025